pH Dependence of the Donor Side Reactions in Ca^{2+}-Depleted Photosystem II†

Stenbjörn Styring,* Yashar Feyziyev, and Fikret Mamedov

Department of Biochemistry, Centre for Chemistry and Chemical Engineering P.O. Box 124, Lund University, S 221 00 Lund, Sweden

Warwick Hillier* and Gerald T. Babcock

Department of Chemistry, Michigan State University, East Lansing, Michigan 48824

Received October 18, 2002; Revised Manuscript Received February 5, 2003

ABSTRACT: We have studied how low pH affects the water-oxidizing complex in Photosystem II when depleted of the essential Ca^{2+} ion cofactor. For these samples, it was found that the EPR signal from the $Y_Z^\bullet$ radical decays faster at low pH than at high pH. At 20 °C, $Y_Z^\bullet$ decays with biphasic kinetics. At pH 6.5, the fast phase encompasses about 65% of the amplitude and has a lifetime of ∼0.8 s, while the slow phase has a lifetime of ∼22 s. At pH 3.9, the kinetics become totally dominated by the fast phase, with more than 90% of the signal intensity operating with a lifetime of ∼0.3 s. The kinetic changes occurred with an approximate pK_a of 4.5. Low pH also affected the induction of the so-called split radical EPR signal from the $S_2Y_Z^\bullet$ state that is induced in Ca^{2+}-depleted PSII membranes because of an inability of $Y_Z^\bullet$ to oxidize the S_2 state. At pH 4.5, about 50% of the split signal was induced, as compared to the amplitude of the signal that was induced at pH 6.5−7, using similar illumination conditions. Thus, the split-signal induction decreased with an apparent pK_a of 4.5. In the same samples, the stable multiline signal from the S_2 state, which is modified by the removal of Ca^{2+}, was decreased by the illumination to the same extent at all pHs. It is proposed that decreased induction of the $S_2Y_Z^\bullet$ state at lower pH was not due to inability to oxidize the modified S_2 state induced by the Ca^{2+} depletion. Instead, we propose that the low pH makes $Y_Z^\bullet$ able to oxidize the S_2 state, making the $S_2 \rightarrow S_3$ transition available in Ca^{2+}-depleted PSII. Implications of these results for the catalytic role of Ca^{2+} and the role of proton transfer between the Mn cluster and Y_Z during oxygen evolution is discussed.

Photosystem II (PSII)[1] is a large membrane-spanning, protein complex comprised of some 30 polypeptide subunits that catalyzes a light-driven charge separation event in the thylakoid membrane, the reduction of plastoquinone, and the oxidation of water to molecular oxygen (*1*−*3*). Recently, two structures of the oxygen-evolving core of PSII at ∼3.8 Å resolution have appeared from *Thermosynechococcus elongatus* (*4*) and *Thermosynechococcus vulcanus* (*5*). These structures have revealed the precise location of several of the redox-active components in PSII. However, much interest and uncertainty still is associated with the oxygen evolving complex (OEC) subdomain of PSII, as there continue to be many details concerning the coupled electron-transfer events and chemistry of O−O bond formation that are not known. What is established is that the OEC contains a cluster of four Mn atoms and a redox-active tyrosine residue, Y_Z, that is situated ∼10 Å away (*4*−*8*). The Mn atoms are suggested to be linked via oxo- and carboxyl-bridges (*9*, *10*), forming a structure ∼6.8 × 4.9 × 3.3 Å in dimension (*4*). One Ca^{2+} ion (*11*), and possibly several Cl^- ions, are also needed for the oxidation of water (*12*, *13*) and are yet to be localized in the X-ray structure.

The oxidation of water by PSII is a cyclic reaction that involves the accumulation of four oxidizing equivalents and then the concerted four-electron oxidation of two water molecules to molecular oxygen. This process is coupled to the reduction of $P680^+$ and the formation of the neutral radical state of the tyrosine, $Y_Z^\bullet$. This radical is detectable by EPR spectroscopy (*1*, *13*−*15*). The oxidized neutral tyrosine $Y_Z^\bullet$ is simultaneously deprotonated to the neighboring D1-His190 residue, which serves as the proton acceptor (*16*−*21*). The coupling of the four-electron water oxidation reaction to the one-electron charge separation events of the reaction center is then achieved with the accumulation of oxidizing equivalents within the OEC that cycles through five intermediate states (S_n, $n = 0-4$) (*22*). The S_0 state is the most reduced intermediate, while the S_4 state is essentially

† This work was supported by the Swedish Natural Science Research Council, the Fulbright Foundation (S.S.), the Royal Physiographic Society in Lund (S.S.), DESS, the Knut and Alice Wallenberg Foundation, the Swedish Energy Administration, and NIH Grant GM37300 (G.T.B.).

* Correspondence should be addressed to the following authors. (W.H.) Ph.: (517) 355-9715. Fax: (517) 353-1793. E-mail: Hillier@photon.cem.msu.edu. (S.S.) Ph.: +46-46 222 0108. Fax: +46-46 222 4534. E-mail: Stenbjorn.Styring@biokem.lu.se.

[1] Abbreviations: Chl, chlorophyll; Cyt, cytochrome; EPR, electron paramagnetic resonance; EGTA, ethylenbis(oxyethylenenitrilo) tetraacetic acid; HEPES, 4-(2-hydroxyethyl)-piperazineethanesulfonic acid; MES, 4-morpholine ethanesulfonic acid; P680, the primary electron donor in PSII; OEC, oxygen evolving complex; PPBQ, *p*-phenyl benzoquinone; PSII, Photosystem II; Y_D, the redox active tyrosine residue D2-161 in PSII that gives rise to the EPR Signal II_{slow}; Y_Z, the redox active tyrosine residue D1-161 that is the immediate electron donor to $P680^+$.

10.1021/bi027035r CCC: $25.00
Published on Web 05/02/2003

a transition state that deactivates immediately to S_0, liberating O_2.

The exact redox changes involved in the S-cycle are controversial. It is generally agreed that both the $S_0 \rightarrow S_1$ and $S_1 \rightarrow S_2$ transitions involve oxidation of Mn ions in OEC; however, the $S_2 \rightarrow S_3$ transition is more controversial, and Mn oxidation, substrate oxidation, or ligand oxidation have been proposed to occur, based on different experimental techniques (*9*, *10*, *23*−*28*). The redox steps of the S cycle also accompany release of four protons from the two water molecules (*29*, *30*). It is debated exactly how this occurs on a molecular level, and essentially, two models dominate the discussion at present. We have advocated a model where $Y_Z^\bullet$ catalyzes a hydrogen-atom transfer from water bound to the Mn cluster on each S cycle transition (*31*−*35*). In the hydrogen-atom transfer mechanism, electron-transfer and proton-transfer reactions are concerted. The protons are expelled from Y_Z immediately upon the oxidation of Y_Z, through a hydrogen-bond network involving D1-His190. This mechanism is energetically favorable, as the reduction of $Y_Z^\bullet$ is charge neutral and proceeds in the same way for every step in the cycle (*36*, *37*). In contrast to this model, mechanistic proposals exist that invoke either pure electron transfer from and to Y_Z or proton-coupled electron transfer (*38*−*43*). In most of these mechanistic proposals, $Y_Z^\bullet$ first deprotonates to its H^+ acceptor, D1-His190, and then during the reduction phase, the proton returns to the tyrosine in the hydrogen bond. The protons from water leave the Mn cluster through a different, ill-defined pathway not involving Y_Z.

It is not clear how the mechanisms of concerted versus coupled electron transfer might be resolved. One cofactor that might provide useful insight into water oxidation chemistry is the Ca cofactor. The OEC can be reversibly depleted of its Ca^{2+} cofactor and is inhibited of O_2 evolution activity. The O_2 evolution can be reconstituted by Ca^{2+} and partially with Sr^{2+} ions (*44*−*48*). The molecular function and location of Ca^{2+} within the OEC are not entirely clear. Several proposals have suggested that the Ca^{2+} ion may be directly involved in O_2 formation by coordinating the substrate water in the S_3 state and facilitating formation of the O−O bond (*26*, *39*, *41*, *49*). It may also serve as a substrate-loading site to catalytic Mn ions, as the measured substrate water-exchange rates in the S_3 state are slow as compared to rates expected of Ca^{2+} (*50*, *51*). A role for Ca^{2+} may also involve proton currents in the OEC, as Ca^{2+} depletion alters the proton-release pattern in the S cycle (*52*, *53*). Removal of Ca^{2+} also results in perturbation of the S_2 state and a block in the S cycle. The S_2 state in Ca^{2+}-depleted PSII gives rise to a very stable, modified S_2 multiline EPR signal from the Mn cluster (*47*, *48*, *52*, *54*). In addition, the OEC stalls in the $S_2Y_Z^\bullet$ state during illumination. The $S_2Y_Z^\bullet$ state also gives rise to a characteristic split EPR signal, observable at low temperature, and $Y_Z^\bullet$ in this state is very long-lived (*6*, *52*, *54*−*58*).

The EPR signals arising from Ca^{2+}-depleted samples therefore provide a useful means to study the inhibited state and also the means to study alleviation of inhibition. We recently reported that the normal S_3 state gave rise to a split EPR signal probably also originating from $S_2Y_Z^\bullet$ when the pH was raised in the S_3 state (*59*). It was proposed that S_3 was converted to $S_2Y_Z^\bullet$ at high pH because of the decreased redox potential of the $Y_Z^\bullet/Y_Z$ couple making Y_Z available for oxidation by the Mn cluster in the S_3 state. It follows, from this proposal, that the redox potential of $Y_Z^\bullet$ is tuned by the pH in the surroundings of PSII. It was also proposed (*59*) that Ca^{2+} depletion could induce a similar situation involving a proton deficiency at the Mn site. Such a proton deficiency in the $(Mn)_4-Y_Z$ environment could lower the oxidizing ability of $Y_Z^\bullet$. This would inhibit turnover between S_2 and S_3, since the S_2 state would become more oxidizing than $Y_Z^\bullet$. An alternative way to see this is that a proton deficiency in the Mn cluster/substrate water ensemble could prevent reduction of $Y_Z^\bullet$, since this reduction demands the arrival of a proton and an electron at the same time. A way to test this is to investigate the behavior of $Y_Z^\bullet$ and the split $S_2Y_Z^\bullet$ EPR signal in Ca^{2+}-depleted PSII at low pH. Here, we report our results from such experiments.

MATERIALS AND METHODS

PSII Preparation. The PSII-enriched membranes (BBY particles) were prepared from market spinach or from hydroponically grown, greenhouse spinach (*60*). The isolated BBY particles were suspended in 50 mM MES-NaOH (pH 6.2), 15 mM NaCl, 5 mM $MgCl_2$, and 400 mM sucrose, which is our standard buffer, at a Chl concentration of 6−10 mg/mL and stored at −80 °C until use.

Depletion of Ca^{2+} from the PSII-Enriched Membranes. Ca^{2+} was removed from PSII by treatment at low pH (pH 3.0 for 5 min at 0 °C) in the presence of 20 mM citrate (*45*). After the Ca^{2+}-depletion treatment, the membranes were first washed with standard buffers (in the presence of 100 μM EGTA) to remove the citrate. The Ca^{2+}-depleted membranes were then washed twice with and finally dissolved in a low-buffering medium (0.25 mM MES-NaOH pH 6.1, 15 mM NaCl, and 400 mM sucrose) to allow the pH jump experiments. The Ca^{2+}-depleted samples exhibited very low (0−10% of the control activity, which was 400−450 μmol of O_2/mg of Chl × h) steady-state oxygen evolution in the absence of Ca^{2+}. In the presence of 20 mM $CaCl_2$, the oxygen evolution was restored to 75−80% of the control oxygen evolution. This is normal for a preparation of Ca^{2+}-depleted PSII, and the lowered maximal oxygen evolution after Ca^{2+} depletion is normally not because of loss of the Mn cluster (*6*, *45*, *47*, *48*, *57*, *61*). Instead, this level of recovery indicates that almost all PSII centers in our preparation contain a fully functional OEC that has lost its Ca^{2+} ion.

pH Jump in the PSII-Enriched Membranes. The Ca^{2+}-depleted membranes in the low-buffering medium were transferred to EPR tubes at a concentration of 4.8 mg Chl/mL. The samples were illuminated with room light for 1 min to allow induction of the stable S_2 state and then dark adapted for 5 min (*45*, *47*, *48*, *54*). Then, the pH was changed by the addition of stronger buffer solutions in the pH range from 3.5 to 7.0: DL-glutamic acid/KOH (pH 4.0−5.0), MES/NaOH (pH 5.0−6.5), and HEPES/NaOH (pH 6.5−7.5). The final buffer concentration was 14 mM. The final pH was measured in each individual sample when all measurements were terminated. To facilitate quick and thorough mixing, the buffers were added and mixed with a syringe, with a spiral-shaped needle inserted directly into the EPR tube (*62*). All procedures, after the room-light illumination, were carried out in darkness. It should be emphasized that all samples were treated in exactly the same way; thus, samples at pH

6−6.5 were also prepared by the addition of more concentrated buffer to the weakly buffered samples.

Induction of the $S_2Y_Z^\bullet$ Signal. Maximal induction of the $S_2Y_Z^\bullet$ EPR signal was achieved by illumination at 0 °C in the presence of 0.5 mM PPBQ as external electron acceptor. The EPR samples were illuminated for 30 s, using scattered heat-filtered white light from an 800 W lamp source (>300 μE/m^2 s at the sample level to avoid photoinhibitory effects), and then the samples were frozen within 1−2 s in a solid CO_2/ethanol bath before they were transferred to liquid nitrogen. This protocol is known to induce almost complete conversion to the $S_2Y_Z^\bullet$ state (*6*, *47*, *48*, *52*, *54*, *63*). We also induced the $S_2Y_Z^\bullet$ state by illumination with the same lamp at 253 K for 2 min or by illumination with five saturating laser flashes at 0 °C (from a Nd:YAG laser, 532 nm, 250−300 mJ) to test if our results were affected by the illumination regime. For the quantification, we measured the amplitude of the low-field maximum of the split EPR signal from $S_2Y_Z^\bullet$.

EPR Spectroscopy. Room-temperature kinetic EPR measurements were performed with a Bruker ESP300 spectrometer equipped with a standard Bruker 4102 cavity. Low-temperature EPR measurements were performed with a Bruker E500 spectrometer using a SuperX ER049X microwave bridge equipped with a Bruker ER 4122SHQ cavity and a liquid-helium cryostat and temperature controller from Oxford Instruments Ltd.

Kinetic Measurements of the Flash-Induced EPR Signal from $Y_Z^\bullet$. For EPR studies of the flash-induced kinetics of $Y_Z^\bullet$, a flat sample cell was used with the Ca^{2+}-depleted PSII membranes at a concentration of about 2 mg Chl/mL. No exogenous electron acceptor was used in these experiments. Exciting flashes to induce the radical EPR signal from $Y_Z^\bullet$ (7 ns, 532 nm, 250−300 mJ) were provided directly into the EPR cavity from a frequency-doubled Nd:YAG laser. In some experiments, 20 mM $CaCl_2$ was added to the samples to allow determination of how large a fraction of PSII was reversibly deprived of Ca^{2+}. In this case, PSII was incubated with $CaCl_2$ for 2 min prior to the EPR measurements, which took about 25 min to conclude. The kinetic EPR measurements were performed at a fixed-field position that corresponds to the low-field maximum of the EPR signal from $Y_Z^\bullet$ as in refs *58* and *64*.

In Ca^{2+}-depleted PSII, $Y_Z^\bullet$ has been reported to have a decay half time of nearly 10 s in the absence of electron acceptors (*58*, *64*). To allow complete decay of $Y_Z^\bullet$ between the repetitive flashes, we used a 1-min dark interval in our experiments. Y_Z and the OEC are very light sensitive in Ca^{2+}-depleted PSII, and they are rapidly damaged through donor-side induced photoinhibition. Only 20 flashes were given to each individual sample in our experiments, to control possible photoinhibition effects. Thereafter, the sample was exchanged for a new sample at the appropriate pH.

In each sample, the dark stable EPR signal from the $Y_D^\bullet$ radical was measured before and after the flashes. To determine the fraction of flash-induced $Y_Z^\bullet$, its amplitude was compared to the amplitude of the $Y_D^\bullet$ radical that amounts to 1-radical spin per PSII center (*1*, *6*, *14*). This comparison was carried out with the ESR300 software package. The radical EPR signals from $Y_D^\bullet$ or $Y_Z^\bullet$ did not change during our experimental protocol that included two measurements of the $Y_D^\bullet$ radical and the accumulation of 20 flash-induced transients from $Y_Z^\bullet$ in each sample. The kinetic fitting of the radical decay kinetics was done using two exponential decay components.

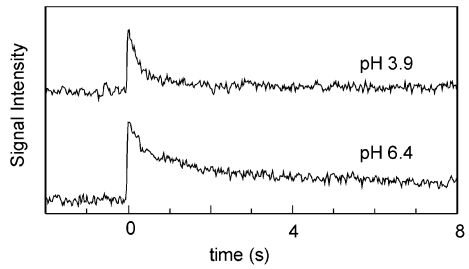

FIGURE 1: Kinetic traces of the induction and decay of the flash-induced EPR signal from $Y_Z^\bullet$ in Ca-depleted PSII membranes at different pH. Experimental conditions: PSII concentration 2.2 mg Chl/mL, sample temperature 293 K, microwave frequency 9.78 GHz, microwave power 20 mW, modulation amplitude 5 G, and conversion time 20 ms. The induction kinetics were averaged for 20 flashes provided with a dark interval between each flash of 1 min. The magnetic field for the measurement was set at the maximum of the low-field peak of $Y_Z^\bullet$ (*64*).

RESULTS

The $Y_Z^\bullet$ radical is very long-lived at room temperature in Ca^{2+}-depleted PSII (*58*, *64*, *65*). Here, we studied the decay of the $Y_Z^\bullet$ radical as a function of pH. Figure 1 shows the first part of decay of the flash-induced EPR signal from $Y_Z^\bullet$ at pH 3.9 and 6.4. The decay of $Y_Z^\bullet$ follows two lifetimes, one faster and one slower. The relative amplitudes of the fast and slow phase appear to be pH dependent. At pH 6.4, the slow phase is clearly visible and encompasses a large fraction of $Y_Z^\bullet$. At pH 3.9, the $Y_Z^\bullet$ signal almost entirely decays in a much faster reaction. The same amount of $Y_Z^\bullet$ was induced by a single flash at both pHs; hence, the amplitude of the flash-induced signal was pH independent. The amplitude of the flash-induced $Y_Z^\bullet$ signal encompassed 20 ± 3% of the total Y_Z, as determined by comparison with the EPR signal from $Y_D^\bullet$ that amounts to one radical per PSII center. In essence, the biphasic decay of $Y_Z^\bullet$ and the amount of the flash-induced radical we find here at pH 6.4 are similar to those reported earlier at this pH (*58*, *64*). The increased decay rate at lower pH and the pH dependence of the relative amplitude of the two decay phases have not been studied before.

In the presence of 20 mM $CaCl_2$, 30−35% of the flash-induced signal of $Y_Z^\bullet$ remained (not shown). This is similar to what has been observed earlier in this kind of Ca^{2+}-depleted PSII (*64*) and corresponds to 7−10% of all PSII centers. This fraction was independent of the measuring pH. The Ca^{2+}-insensitive centers most likely represent PSII centers that have lost their Mn cluster in the preparation procedures. The decay of $Y_Z^\bullet$ of this fraction of centers is faster at low pH and is quite similar to that in Tris-washed PSII centers that lack the Mn cluster (*66*, *67*). The remaining 65−70% of the flash-induced signal from $Y_Z^\bullet$ disappeared in the presence of Ca^{2+}, indicating that the OEC could be reactivated in these PSII centers.

Similar flash experiments, intended to follow the induction and decay of the EPR signal from $Y_Z^\bullet$, were conducted between pH 3.9 and 7. Figure 2 shows the pH dependence of the decay kinetics $Y_Z^\bullet$ obtained by fitting of kinetic decay traces similar to those in Figure 1 with a Henderson−

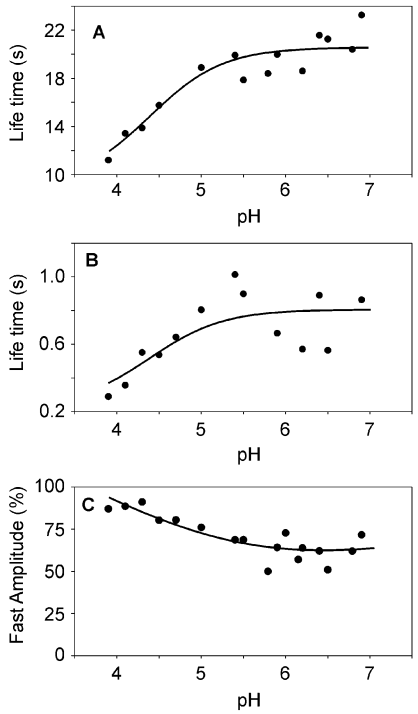

FIGURE 2: Flash-induced $Y_Z^\bullet$ decay components in Ca^{2+}-depleted PSII membranes as a function of pH. The slow (A) and fast (B) decay kinetics and the amplitude of the fast phase (C) were obtained by biexponential fit of data recorded as in Figure 1. The pH profiles (A) and (B) were determined from a fit using the combined data and derived an apparent pK_a of 4.4 ± 0.2.

Hasselbalch equation. Both the slow- and fast-decay phases are pH dependent, and both phases become faster at lower pH. At pH 6.4, the fast phase decays with 0.8 s and the slow phase with 22 s lifetimes, respectively. At pH 3.9, the lifetimes for the decay of $Y_Z^\bullet$ are 0.3 and 11 s for the fast and slow phases, respectively. Figure 2C shows how the relative amplitudes of the fast phase are modified by pH. Between pH 6.4−7.0, about 65% of $Y_Z^\bullet$ decays with fast kinetics (lifetime 0.8 s), while the remaining fraction decays 25−30 times slower (lifetime about 20 s). At pH 3.9, however, the fast phase dominates completely. It encompasses about 90% of $Y_Z^\bullet$, while only about 10% decays with the slow kinetics (which, consequently, are difficult to determine with precision).

The data in Figure 2 also contain information about at which pH the changes occur that led to the faster decay of $Y_Z^\bullet$. Above pH 6, the two decay phases are quite insensitive to the pH. Both decay phases start to become faster below pH ~5−5.5. We have not measured below pH 3.9, but at this pH, the slow phase should almost be absent. Fitting the two data sets together to determine a common apparent pK_a derived a value of 4.4. However, as apparent within the data, an additional component(s) may influence this apparent pK_a.

The kinetic-decay traces for $Y_Z^\bullet$ were recorded at room temperature and indicate that the pH had substantial effects on the behavior of $Y_Z^\bullet$. We, therefore, performed trapping experiments to investigate the effect of pH on the induction of the $S_2Y_Z^\bullet$ split EPR signal that can be induced by illumination around 0 °C in Ca^{2+}-depleted PSII (*45*, *47*, *48*, *54*). In this experiment (Figures 3 and 4), the Ca^{2+}-depleted PS membranes were pre-illuminated at standard pH to induce the stable S_2 state that is typical for Ca^{2+}-depleted PSII.

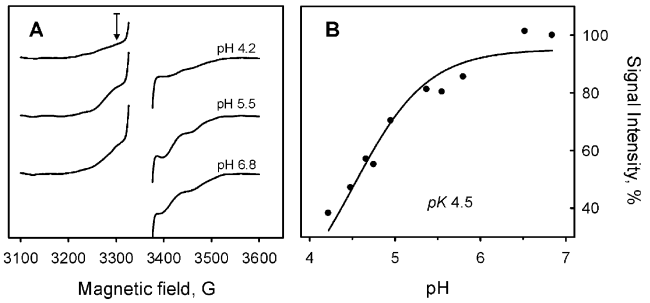

FIGURE 3: (A) EPR spectra of the split EPR signal from the S_2 $Y_Z^\bullet$ state. The signal was induced at different pHs by illumination of Ca^{2+}-depleted PSII for 30 s at 0 °C. The arrow indicates the field position chosen for the measurements of the amplitude of the signal, which was measured from the top of the signal shoulder (at 3300 G) to the baseline. EPR conditions: temperature 10 K, microwave frequency 9.41 GHz, microwave power 20 mW, and modulation amplitude 10 G. (B) pH dependence of the amplitude of the S_2 $Y_Z^\bullet$ signal (measured as in panel A) and fitting of the signal amplitude to a pH dependence with a single pK_a of 4.5.

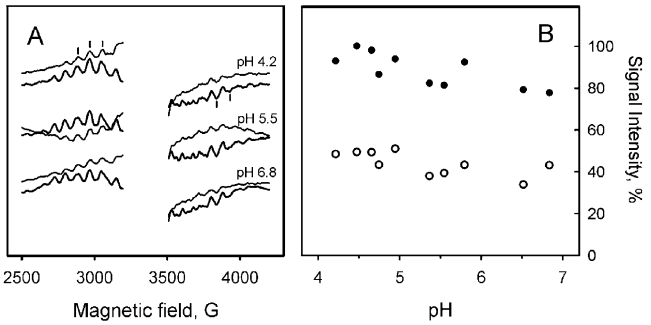

FIGURE 4: (A) EPR spectra of the stable S_2 multiline signal in the Ca^{2+}-depleted PSII membranes at different pH values before (black) and after illumination at 0 °C for 30 s (grey). The spectra are recorded in the same samples as the split signal in Figure 3. The large signals from $Y_D^\bullet$ and the split S_2 $Y_Z^\bullet$ are removed from the middle of the spectra to facilitate comparison of the multiline spectra. EPR conditions, as in Figure 3. The bars indicate the peaks chosen for the measurements of the amplitude of the signal. (B) pH dependence of the amplitude of stable S_2 multiline signal recorded before (●) and after (○) illumination at 0 °C for 30 s.

Thereafter, the samples were subjected to a pH jump (*59*), and the multiline signal from the stable S_2 state was measured (Figure 4). Then the samples were thawed and illuminated for 30 s at 0 °C and then rapidly frozen. It is important to note that this illumination protocol, in our hands, leads to maximal changes in the both the stable multiline signal and the split signals (not shown, see also below). Figure 3A shows the induction of the split signal from $S_2Y_Z^\bullet$ at three different pHs. At pH 6.8, the signal was large and easily detectable. At lower pH, the signal becomes smaller at pH 4.2, the amplitude was less than half of that at pH 6.8. The pH dependence of the induction of the signal is shown in Figure 3B. The maximum is at pH 6.5−7.0, and the signal becomes progressively smaller toward low pH. The pK_a for the decrease of the $S_2Y_Z^\bullet$ signal is about 4.5, which is close to the pH where the changes in the $Y_Z^\bullet$ kinetics occurred (compare with Figure 2).

The $S_2Y_Z^\bullet$ signal in the experiment shown in Figure 3 was induced by 30 s illumination at 0 °C, which we found to induce the largest split signal in the range of pH 6−7. Longer illumination did not increase the yield of the signal. It is possible, however, that this illumination protocol was not optimal at lower pHs or possibly it might have induced

photoinhibition. We, therefore, tested how pH affected the induction of the $S_2Y_Z^\bullet$ signal, by a series of powerful laser flashes at 0 °C or by illumination at 253 K, to test if these illumination protocols (which both exclude the photoinhibition problem) would affect the yield of the signal. However, neither of these illumination regimes (results not shown) changed the pH dependence for the induction of the $S_2Y_Z^\bullet$ signal that is shown in Figure 3. The signal intensity at pH 4.5 was always about 50% of the signal amplitude induced at pH 6.5−7. Therefore, we conclude that the lowered signal intensity at low pH was not due to altered light dependence or temperature dependence for the induction of the $S_2Y_Z^\bullet$ signal. Instead, the chemistry behind the lower induction of the signal probably reflects the mechanism behind the induction of the $S_2Y_Z^\bullet$ state in Ca^{2+}-depleted PSII membranes.

We also tested how the S_2 state in the Ca^{2+}-depleted membranes behaved during illumination at the different pHs. In Ca^{2+}-depleted PSII, the S_2 state is abnormally stable and gives rise to a modified multiline EPR signal. This can vary in size, depending on the preparation procedure and the buffers used in the experiment (*68*). In our preparation, the S_2 multline EPR signal in this state was clearly visible at all pHs (Figure 4A, black spectra). The signal shape was pH independent, and the amplitude decreased only very slightly (10−20%) at high pH values (Figure 4B). After the illumination, at least 50% of the stable multiline signal was lost at all pHs (Figure 4A, gray spectra; Figure 4B). In our amplitude analysis, only the most prominent signal peaks were used (marked in Figure 4A). Some other peaks were completely lost during the illumination procedure. Therefore, the actual decrease of the stable multiline signal might be higher than 50%. The most important result of this experiment is that the stable multiline signal disappeared in a pH independent manner during illumination at 0 °C.

Interestingly, the amplitude of the stable S_2 multiline signal is almost independent of pH (Figure 4B). This finding is different from the behavior of the multiline EPR signals for the normal S_2 state and the S_0 state, which both exhibit decreased amplitudes at acidic and alkaline pHs (*62*). The reason for this difference is unknown, at present.

Several components in PSII are known to compete with Y_Z as electron donor to $P680^+$. The most studied are Cytb_{559}, a chlorophyll molecule known as Chl_Z, and a carotenoid molecule (*1*, *14*, *69*−*72*). These alternative electron donors have not been observed to function in this temperature interval in the presence of the Mn cluster. We, nevertheless, checked their participation by EPR measurements in our samples (not shown). There was always some (less than 10%) induction of a Chl radical in Ca^{2+}-depleted PSII during illumination at 0 °C, but there was no trace of any increased induction of the radical EPR signals from Chl or carotenoid at low pHs in the samples studied in Figure 3. Furthermore, there are no signs of enhanced light-dependent oxidation of Cytb_{559} at the lower pHs where we have the diminished induction of the $S_2Y_Z^\bullet$ signal (Figure 3).

DISCUSSION

Depletion of Ca^{2+} from PSII inhibits steady-state oxygen evolution reversibly because of an interruption in the S cycle between the S_2 and the S_3 states. The reason for this interruption may relate to the disruption of proton currents within the OEC. Specifically, it has been proposed that the reduction of $Y_Z^\bullet$ operates under a regime where coupled and concerted electron and proton transfer occurs (*31*, *32*, *34*−*36*). Therefore, as a consequence of disruption to proton movement the thermodynamics of the reaction would change, and electron transfer would be prevented. It turns out that there is no proton release from Ca^{2+}-depleted PSII centers during this transition in our type of PSII-enriched membranes (*52*). This is potentially indicative of perturbations to proton movements. The S_2 state is also altered in Ca^{2+}-depleted PSII (*13*, *47*, *48*, *54*). The spectral shape of the S_2 multiline EPR signal is modified by the removal of Ca^{2+}, and the S_2 state is rendered much more stable than in fully functional PSII. The changes induced by Ca^{2+} depletion also directly involve the $Y_Z^\bullet$ state, which becomes unable to oxidize the modified S_2 state and leads to the formation of an interesting spin-coupled EPR signal, denoted the split signal. This was early recognized to originate from a radical in close magnetic interaction with the Mn cluster in the S_2 state (*52*, *61*). In acetate-inhibited PSII, the radical was subsequently identified as $Y_Z^\bullet$ (*55*). The signal is now known as the $S_2Y_Z^\bullet$ EPR signal.

Despite such intensive studies, the field has not resolved a functional versus structural role for Ca in the water oxidation reaction. Part of this stems from uncertainty of the location of the Ca ion (*73*−*75*). We decided to investigate the Ca^{2+}-depleted system with a series of pH experiments and show that the pH in the bulk medium has large effects on subtle probes to the photochemistry in Ca^{2+}-depleted PSII. Our findings show that the $Y_Z^\bullet$ radical decays much faster at low pH than at high pH. Furthermore, the amplitude of the $S_2Y_Z^\bullet$ signal is decreased by low pH in the medium.

We see several potential mechanisms that can give rise to these pH-dependent effects. First, the loss of the split signal at low pH may result from changes in the magnetic coupling between the Mn cluster and $Y_Z^\bullet$. Such changes could arise from changes in geometry. However, the amplitudes of both stable multiline signal and $Y_Z^\bullet$ are unaffected by pH changes, and it is speculative to invoke that pH-induced changes in the magnetic interaction affect the kinetics of $Y_Z^\bullet$. A second possibility is $Q_A^-/Y_Z^\bullet$ recombination is pH dependent, becoming faster at low pH in PSII centers depleted of the Mn cluster (*19*, *66*, *67*) because of increases in driving force (ΔG) for the recombination reaction. The energetic change would unlikely be associated with Q_A redox reactions that are not linked to proton-transfer yet may involve Y_Z, which itself must be reprotonated on reduction. Perturbation or blockage of the hydrogen-bonding network around Y_Z may prevent recombination taking place (*19*). Thus, an increased recombination rate could indicate that the midpoint potential of the $Y_Z^\bullet/Y_Z$ couple is pH dependent and controlled by the bulk medium. This is not unexpected, as in Tris-washed PSII samples, Y_Z interacts readily with reductants and other agents in the environment, and this seems to be the case in Mn-containing, functional PSII centers (*59*, *76*). Therefore, it is feasible that, in Ca^{2+} depleted PSII, the faster decay of $Y_Z^\bullet$ at low pH could be the result of the direct titration of Y_Z.

However, we also see another explanation of our data. This is built on our observation that, during illumination at 0 °C, the stable S_2 multiline signal is abolished to a larger extent

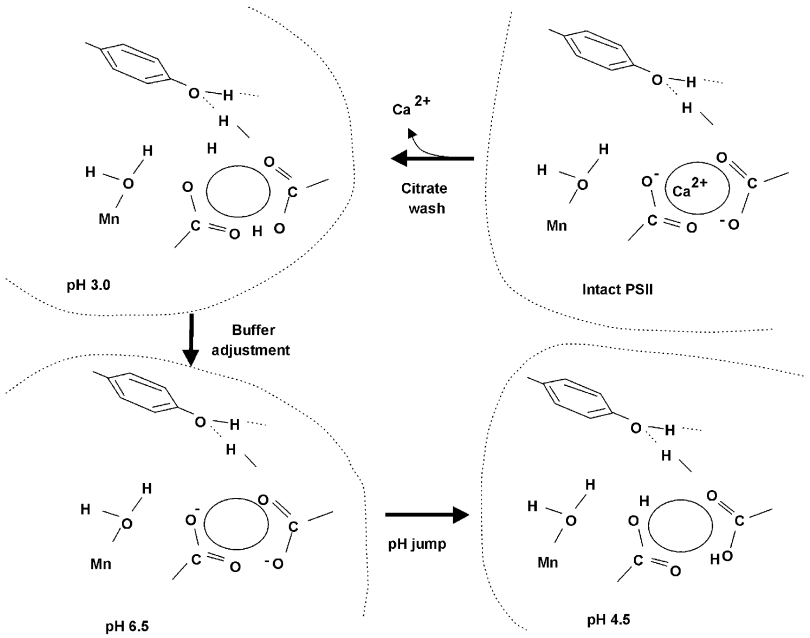

FIGURE 5: Model for the changes of the protonation state in the Mn-Ca-Y_Z environment in our experiments. When intact PSII is washed with citrate at pH 3.0, this removes the Ca^{2+} ion from its site. The carboxylic residues that most probably bind the Ca^{2+} ion (here drawn as two residues, but there is little evidence of how many residues are really involved in the binding of Ca^{2+}) are protonated. When the centers are brought back to normal pH, the carboxylic residues are deprotonated, making the OEC proton deficient. This proton deficiency is proposed to be relieved by low pH, where the carboxylic residues are protonated again. Our results indicate that this occurs with a pK_a ~4.5, which alters the decay kinetics of $Y_Z^\bullet$ and perhaps makes it possible for $Y_Z^\bullet$ to oxidize the S_2 state.

than the $S_2Y_Z^\bullet$ signal is formed at low pH (Figures 3 and 4). Thus, more than 50% of the S_2 population disappears when the Ca^{2+}-depleted PSII centers are illuminated in the entire pH range studied. In contrast, the amplitude of the S_2 $Y_Z^\bullet$ signal at pH 4.5 is only half of the signal amplitude at pH 6−7. This means that a large fraction of the PSII centers (about 20−30%, see Results section) did not form the $S_2Y_Z^\bullet$ intermediate at low pH. Which is then the redox state for those centers? It is unlikely that they did not turn over at all or that $Y_Z^\bullet$ was rapidly lost due to recombination (see above). In both cases, the S_2 state would be the resulting state after the illumination, and an increased fraction of the stable S_2 multiline signal should have remained at lower pH. This was not the case! Probably, we should also have observed oxidation of one or other of the alternative electron donors in PSII in 20−30% of the centers that did not form the $S_2Y_Z^\bullet$ signal. This was not observed! Instead, we propose that the $Y_Z^\bullet$ actually is able to oxidize the S_2 state to the S_3 state at low pH. The system is thus not inhibited in the $S_2Y_Z^\bullet$ state but advances to the S_3 state.

We cannot ascertain if the S cycle stalled after the formation of the S_3 state or if the system can progress even further, since we know of no easily accessible probes to these redox states in the Ca^{2+}-depleted PSII. However, we have recently determined that both the $S_2 \rightarrow S_3$ and the $S_3 \rightarrow S_0$ transitions in intact PSII are blocked with sharp pK_a values of 4.0 and 4.5, respectively (*76*). Thus, it is most likely that PSII stalled in the S_3 state in our experiments. If this analysis holds true, the situation in the Ca^{2+}-depleted PSII is complex at low pH. The effect of the removal of Ca^{2+} might be partially or completely abolished around pH 4, and the S_2 state can now be oxidized by $Y_Z^\bullet$, resulting in the formation of the S_3 state and faster (although still very slow, as compared to functional PSII) decay kinetics for $Y_Z^\bullet$.

Why, then, should the inhibition induced by Ca^{2+} depletion be abolished by low pH? We suggest that this is a consequence of the mechanism for the reduction of $Y_Z^\bullet$. The Ca^{2+} ion in the OEC is most likely bound to one or several carboxylic residues (*77*, *78*), even if these have not yet been conclusively identified (*79*) (Figure 5). When the pH is lowered to pH 3.0 in the Ca^{2+}-depletion procedure, these carboxylic groups become protonated, leading to release of Ca^{2+} from its site. When the pH is increased in the absence of Ca^{2+}, these carboxylic residues will probably become deprotonated (Figure 5). This creates a severe proton deficiency in the OEC in the absence of Ca^{2+}. Consequently, since $Y_Z^\bullet$ reduction demands the coupled transfer of both an electron and a proton from its close environment, the reduction of $Y_Z^\bullet$ is likely to be much slowed (or even completely inhibited). However, when the pH is decreased, the carboxylic groups become protonated again (Figure 5). This eliminates the proton deficiency and allows reduction and the simultaneous protonation of $Y_Z^\bullet$. It is interesting that the pH-induced decrease in the formation of the S_2 $Y_Z^\bullet$ signal and the increased decay rate of $Y_Z^\bullet$ occur with an apparent pK_a of 4.5, which is in the range for the normal titration of carboxylic amino acid side chains. We assume that it reflects the sum of pK_as of at least two residues involved in the Ca^{2+} binding. To conclude, one interpretation of our results is that the inhibition of the oxygen evolution in Ca^{2+}-depleted PSII is due to inability of OEC to provide a proton necessary for the reduction of $Y_Z^\bullet$.

Comparison of the intact PSII and Ca^{2+}-depleted PSII at pH 6.5 (upper right vs lower left in Figure 5) reveals that the Ca^{2+}-depleted system will behave like a proton-deficient site. In the intact system, the carboxylic side chains constituting the Ca^{2+} site are occupied in Ca^{2+} binding. However, in the Ca^{2+}-depleted system, at pH 6.5 these carboxylic groups

are titrated, creating a situation in the site where any produced protons from water are likely to be consumed by the carboxylic side chains.

The option that the hydrogen bonding network involving Y_Z, D1-His190, and their hydrogen bonding partners (as yet not identified) is in direct contact with the bulk medium in Ca^{2+}-depleted PSII membranes is, in itself, interesting. This strengthens a similar conclusion that was recently derived from the observation that the functional S_3 state was converted to the $S_2Y_Z^{\bullet}$ state by a pH jump to pH >8 (*59*). In this paper, it was concluded that the midpoint potential of the $Y_Z^{\bullet}/Y_Z$ redox couple was altered from about +950 mV at pH 6.5 (*80*) to +830 mV at pH 8.5, which is low enough to be oxidized by the S_3 state (*59*). It was also implied that Y_Z was directly titrated from the bulk medium. Thus, together with the earlier study (*59*), our present results would indicate that the hydrogen bonding network involving Y_Z is in direct, kinetically sufficient, contact with the bulk medium in PSII that binds the Mn cluster. This contact is a prerequisite for the H-atom transfer model for water oxidation that demands proton expulsion to bulk accompanying Y_Z oxidation.

The impact of our results on ideas about the hydrogen-bonding situation around $Y_Z^{\bullet}$ and the Mn cluster in Ca^{2+}-depleted PSII should also be discussed. EPR spectroscopic investigations in Ca^{2+}-depleted PSII (*63*, *81*) indicate that $Y_Z^{\bullet}$ is involved in a bifurcated hydrogen bond. Optical investigations (*53*) have also indicated that the hydrogen-bond network around Y_Z is perturbed in Ca^{2+}-depleted PSII core particles. One of the hydrogen-bond partners to Y_z is most likely D1-His190, which is also part of the hydrogen-bond network in intact and Mn-depleted PSII (*17*−*21*). The other hydrogen-bonding partner to $Y_Z^{\bullet}$ is less well-characterized, and its existence has not been ascertained in functional, oxygen-evolving PSII. It was suggested that the results in the Ca^{2+}-depleted PSII in fact reported on the situation in oxygen-evolving PSII, which would indicate that one of the hydrogen bonds from Y_Z would involve substrate water (*63*). This opinion was recently questioned (*53*), and it was concluded that the hydrogen-bonding situation around Y_Z was disturbed in Ca^{2+}-depleted PSII, as compared to fully functional, oxygen-evolving PSII. Our observation that low pH potentially makes $Y_Z^{\bullet}$ able to oxidize the S_2 state in Ca^{2+}-depleted PSII has bearing on these interpretations. Figure 5 summarizes our current ideas on the situation around the Ca-Mn-Y_Z system at normal and high pH. At pH 6.5, the Ca^{2+} site is empty and the carboxylic ligands are deprotonated, making the entire site proton deficient. Although Y_Z is hydrogen bonded to two partners (*63*, *81*), indicated in Figure 5, one proton is expelled upon its oxidation, after which proton expulsion ceases completely (*53*). This would make the system even more proton deficient, resulting in the observed effect that $Y_Z^{\bullet}$ cannot anymore oxidize the S_2 state. A likely reason is that there is no proton available in the OEC to accompany an electron in the reduction step that is needed to reset Y_Z to its original state. In contrast, at pH 4.5, the carboxylic residues in the Ca^{2+} site are protonated to a large extent. Thus, there is no restriction for proton currents to occur between the Mn moiety (and the protonated but metal-deprived Ca^{2+} site) and the oxidized Y_Z.

The possibility to advance to S_3 state in Ca^{2+}-depleted PSII at low pHs reveals the role of Ca^{2+} cofactor in the intact system. It could imply that Ca^{2+} site in PSII is situated close to the proton-conducting pathway, or possibly, close to the water channel. This suggestion requires further investigation.

ACKNOWLEDGMENT

This was work initiated by S. Styring during his sabbatical stay at Michigan State University and was concluded and written for publication posthumously after the death of G. T. Babcock.

REFERENCES

1. Diner, B. A., and Babcock, G. T. (1996) in *Oxygenic Photosynthesis: The Light Reactions* (Yocum, C. F., Ed.) pp 213−247, Kluwer Academic Publishers, Dordrecht, The Netherlands.
2. Barber, J., Nield, J., Morris, E. P., Zheleva, D., and Hankamer, B. (1997) *Phys. Plant. 100*, 817−827.
3. Debus, R. J. (2001) *Biochim. Biophys. Acta 1503*, 164−186.
4. Zouni, A., Witt, H. T., Kern, J., Fromme, P., Krau*β*, N., Saenger, W., and Orth, P. (2001) *Nature 409*, 739−743.
5. Kamiya, N., and Shen, J.-R. (2003) *Proc. Natl. Acad. Sci. U.S.A. 100*, 98−103.
6. Peloquin, J. M., Campbell, K. A., and Britt, R. D. (1998) *J. Am. Chem. Soc. 120*, 6840−6841.
7. Lakshmi, K. V., Eaton, S. S., Eaton, G. R., Frank, H. A., and Brudvig, G. W. (1998) *J. Phys. Chem. B 102*, 8327−8335.
8. Dorlet, P., Di Valentin, M., Babcock, G. T., and McCracken, J. L. (1998) *J. Phys. Chem. B 102*, 8239−8247.
9. Yachandra, V. K., Sauer, K., and Klein, M. P. (1996) *Chem. Rev. 96*, 2927−2950.
10. Carrell, T. G., Tyryshkin, A. M., and Dismukes, G. C. (2002) *J. Biol. Inorg. Chem. 7*, 2−22.
11. Ädelroth, P., Lindberg, K., and Andréasson, L.-E. (1995) *Biochemistry 34*, 9021−9027.
12. Wincencjusz, H., Yocum, C. F., and van Gorkom, H. J. (1998) *Biochemistry 37*, 8595−8604.
13. Debus, R. J. (1992) *Biochim. Biophys. Acta 1102*, 269−352.
14. Miller, A. F., and Brudvig, G. W. (1991) *Biochim. Biophys. Acta 1056*, 1−18.
15. Diner, B. A. (2001) *Biochim. Biophys. Acta 1503*, 147−163.
16. Debus, R. J. (2000) in *Manganese and its role in Biological Processes* (Sigel, H., Ed.) pp 213−247, Marcel Dekker Inc, Basel, Switzerland.
17. Svensson, B., Etchebest, C., Tuffery, P., vanKan, P., Smith, J., and Styring, S. (1996) *Biochemistry 35*, 14486−14502.
18. Svensson, B., Vass, I., Cedergren, E., and Styring, S. (1990) *EMBO J. 9*, 2051−2059.
19. Mamedov, F., Sayre, R. T., and Styring, S. (1998) *Biochemistry 37*, 14245−14256.
20. Hays, A.-M. A., Vassiliev, I. R., Golbeck, J. H., and Debus, R. J. (1998) *Biochemistry 37*, 11352−11365.
21. Hays, A.-M. A., Vassiliev, I. R., Golbeck, J. H., and Debus, R. J. (1999) *Biochemistry 38*, 11851−11865.
22. Kok, B., Forbush, B., and McGloin, M. (1970) *Photochem. Photobiol. 11*, 457−475.
23. Styring, S. A., and Rutherford, A. W. (1988) *Biochemistry 27*, 4915−4923.
24. Ono, T.-a., Noguchi, T., Inoue, Y., Kusunoki, M., Matsushita, T., and Oyanagi, H. (1992) *Science 258*, 1335−1337.
25. Iuzzolino, L., Dittmer, J., Dörner, W., Meyer-Klaucke, W., and Dau, H. (1998) *Biochemistry 37*, 17112−17119.
26. Kuzek, D., and Pace, R. J. (2001) *Biochim. Biophys. Acta 1503*, 123−137.
27. Dau, H., Iuzzolino, L., and Dittmer, J. (2001) *Biochim. Biophys. Acta 1503*, 24−39.
28. Messinger, J., Robblee, J. H., Bergmann, U., Fernandez, C., Glatzel, P., Visser, H., Cinco, R. M., McFarlane, K. L., Bellacchio, E., Pizarro, S. A., Cramer, S. P., Sauer, K., Klein, M. P., and Yachandra, V. K. (2001) *J. Am. Chem. Soc. 123*, 7804−7820.
29. Lavergne, J., and Junge, W. (1993) *Photosynth. Res. 38*, 279−296.
30. Haumann, M., and Junge, W. (1996) in *Oxygenic Photosynthesis: The Light Reactions* (Yocum, C. F., Ed.) pp 165−192, Kluwer Academic Publishers, Dordrecht, The Netherlands.

31. Hoganson, C. W., Lydakis-Simantiris, N., Tang, X.-S., Tommos, C., Warncke, K., Babcock, G. T., Diner, B. A., McCracken, J., and Styring, S. (1995) *Photosynth. Res. 46*, 177−184.
32. Hoganson, C. W., and Babcock, G. T. (1997) *Science 277*, 1953−1956.
33. Hoganson, C. W., and Babcock, G. T. (2000) in *Manganese and its role in Biological Processes* (Sigel, H., Ed.) Marcel Dekker Inc, Basel, Switzerland.
34. Tommos, C., and Babcock, G. T. (1998) *Acc. Chem. Res. 31*, 18−25.
35. Westphal, K. L., Tommos, C., Cukier, R. I., and Babcock, G. T. (2000) *Curr. Opin. Plant Biol. 3*, 236−242.
36. Tommos, C., and Babcock, G. T. (2000) *Biochim. Biophys. Acta 1458*, 199−219.
37. Blomberg, M. R. A., Siegbahn, P. E. M., Styring, S., Babcock, G. T., Åkermark, B., and Korall, P. (1997) *J. Am. Chem. Soc. 119*, 8285−8292.
38. Haumann, M., and Junge, W. (1999) *Biochim. Biophys. Acta 1411*, 86−91.
39. Vrettos, J. S., Limburg, J., and Brudvig, G. W. (2001) *Biochim. Biophys. Acta 1503*, 229−245.
40. Schlodder, E., and Witt, H. T. (1999) *J. Biol. Chem. 274*, 30387−30392.
41. Pecoraro, V. L., Baldwin, M. J., Caudle, M. T., Hsieh, W. Y., and Law, N. A. (1998) *Pure Appl. Chem. 70*, 925−929.
42. Nugent, J. H. A., Rich, A. M., and Evans, M. C. W. (2001) *Biochim. Biophys. Acta 1503*, 138−146.
43. Rappaport, F., and Lavergne, J. (2001) *Biochim. Biophys. Acta 1503*, 246−259.
44. Ghanotakis, D. F., Babcock, G. T., and Yocum, C. F. (1984) *FEBS Lett. 167*, 127−130.
45. Ono, T.-a., and Inoue, Y. (1988) *FEBS Lett. 227*, 147−152.
46. Boussac, A., and Rutherford, A. W. (1988) *Chem. Scr. 28A*, 123−126.
47. Sivaraja, M., Tso, J., and Dismukes, G. C. (1989) *Biochemistry 28*, 9459−9464.
48. Ono, T.-a., and Inoue, Y. (1989) *Biochim. Biophys. Acta 973*, 443−449.
49. Siegbahn, P. E. M., and Crabtree, R. H. (1999) *J. Am. Chem. Soc. 121*, 117−127.
50. Hillier, W., and Wydrzynski, T. (2001) *Biochim. Biophys. Acta 1503*, 197−209.
51. Hillier, W., Hendry, G., Burnap, R. L., and Wydrzynski, T. (2001) *J. Biol. Chem. 276*, 46917−46924.
52. Boussac, A., Zimmermann, J. L., Rutherford, A. W., and Lavergne, J. (1990) *Nature 347*, 303−306.
53. Haumann, M., and Junge, W. (1999) *Biochim. Biophys. Acta 1411*, 121−133.
54. Boussac, A., Zimmermann, J. L., and Rutherford, A. W. (1989) *Biochemistry 28*, 8984−8989.
55. Gilchrist, M. L., Jr., Ball, J. A., Randall, D. W., and Britt, R. D. (1995) *Proc. Natl. Acad. Sci. U.S.A. 92*, 9545−9549.
56. Maclachlan, D. J., and Nugent, J. H. A. (1993) *Biochemistry 32*, 9772−9780.
57. Andréasson, L.-E., Vass, I., and Styring, S. (1995) *Biochim. Biophys. Acta 1230*, 155−164.
58. Lydakis-Simantiris, N., Dorlet, P., Ghanotakis, D. F., and Babcock, G. T. (1998) *Biochemistry 37*, 6427−6435.
59. Geijer, P., Morvaridi, F., and Styring, S. (2001) *Biochemistry 40*, 10881−10891.
60. Berthold, D. A., Babcock, G. T., and Yocum, C. F. (1981) *FEBS Lett. 134*, 231−234.
61. Boussac, A., and Rutherford, A. W. (1988) *Biochemistry 27*, 3476−3483.
62. Geijer, P., Deak, Z., and Styring, S. (2000) *Biochemistry 39*, 6763−6772.
63. Tommos, C., McCracken, J., Styring, S., and Babcock, G. T. (1998) *J. Am. Chem. Soc. 120*, 10441−10452.
64. Andréasson, L. E., Vass, I., and Styring, S. (1995) *Biochim. Biophys. Acta 1230*, 155−164.
65. de Paula, J. C., Li, P. M., Miller, A. F., Wu, B. W., and Brudvig, G. W. (1986) *Biochemistry 25*, 6487−94.
66. Yerkes, C. T., Babcock, G. T., and Crofts, A. R. (1983) *FEBS Lett. 158*, 359−363.
67. Shigemori, K., Mino, H., and Kawamori, A. (1997) *Plant Cell Physiol. 38*, 1007−1011.
68. Boussac, A., Zimmermann, J. L., and Rutherford, A. W. (1990) *FEBS Lett. 277*, 69−74.
69. Whitmarsh, J., and Pakrasi, H. B. (1996) in *Oxygenic photosynthesis: The Light reactions* (Yocum, C. F., Ed.) pp 249−264, Kluwer Academic Press, Dordrecht, The Netherlands.
70. Thompson, L. K., Miller, A. F., Buser, C. A., Depaula, J. C., and Brudvig, G. W. (1989) *Biochemistry 28*, 8048−8056.
71. Hanley, J., Deligiannakis, Y., Pascal, A., Faller, P., and Rutherford, A. W. (1999) *Biochemistry 38*, 8189−8195.
72. Tracewell, C. A., Cua, A., Stewart, D. H., Bocian, D. F., and Brudvig, G. W. (2001) *Biochemistry 40*, 193−203.
73. Cinco, R. M., Robblee, J. H., Rompel, A., Fernandez, C., Yachandra, V. K., Sauer, K., and Klein, M. P. (1998) *J. Phys. Chem. B 102*, 8248−8256.
74. MacLachlan, D. J., Nugent, J. H. A., and Evans, M. C. W. (1994) *Biochim. Biophys. Acta 1185*, 103−111.
75. Riggs-Gelasco, P. J., Mei, R., Ghanotakis, D. F., Yocum, C. F., and Penner-Hahn, J. E. (1996) *J. Am. Chem. Soc. 118*, 2400−2410.
76. Bernat, G., Morvaridi, F., Feyziyev, Y., and Styring, S. (2002) *Biochemistry 41*, 5830−5843.
77. Noguchi, T., Ono, T.-a., and Inoue, Y. (1995) *Biochim. Biophys. Acta 1228*, 189−200.
78. Qian, M., Dao, L., Debus, R. J., and Burnap, R. L. (1999) *Biochemistry 38*, 6070−6081.
79. Kimura, Y., and Ono, T. A. (2001) *Biochemistry 40*, 14061−14068.
80. Vass, I., and Styring, S. (1991) *Biochemistry 30*, 830−839.
81. Force, D. A., Randall, D. W., and Britt, R. D. (1997) *Biochemistry 36*, 12062−12070.

BI027035R